Present-Day Tectonic Deformation Across Tianshan From Satellite Geodetic data (Dragon Project 59308)

Jiangtao_Qiu[1,2], Jianbao Sun[1]

1: Institute of Geology, China Earthquake Administration, China; 2: The Second Monitoring and Application Center, China Earthquake Administration, China

Introduction

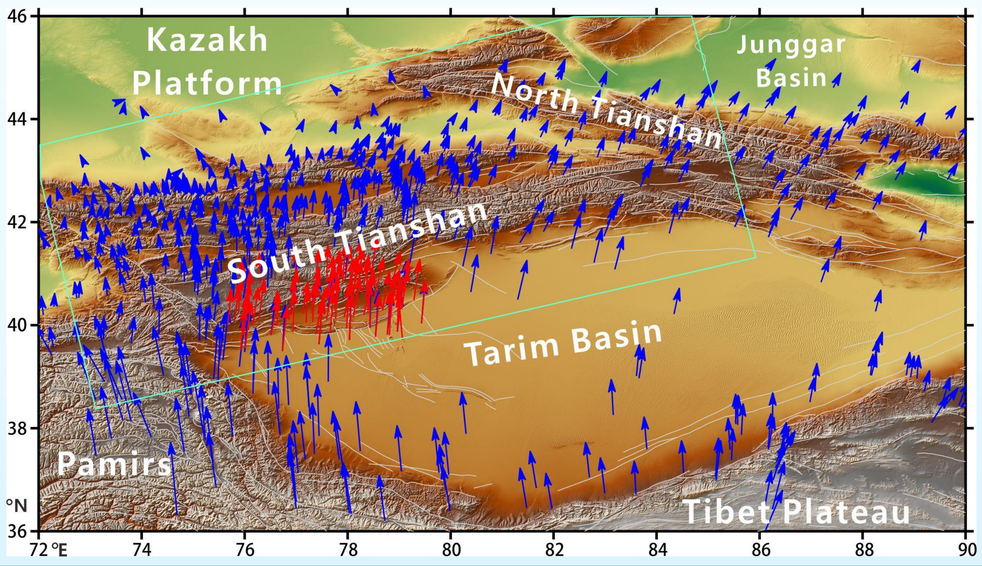

The Tianshan orogenic belt (TSOB) stands as one of Eurasia's most dynamically active regions. The far-range effects of the collision between the Indian and the Eurasian plates in the late Cenozoic led to the reactivation of the TSOB and the intracontinental orogeny. Simultaneously, the TSOB expanded to the foreland basins on its both flanks, forming multiple rows of décollement- and fault-related folds within the basin-mountain transition zone. GPS observations reveal a gradual reduction in the north-south shortening rate across the TSOB, declining from approximately 20 mm/year in the west to around 8 mm/year in the east. Nevertheless, the internal distribution of deformation within the TSOB remains a subject of debate. In this study, we ascertain the present-day kinematics of the primary structural belts through an analysis of geodetic data (GPS & InSAR).

Figure 1. Topography, tectonic settings and GPS velocities in our study area (light green frame) and its surroundings. MDF: Maidan fault, KTF: kepingtag fault, KGF: Kongur fault, PFT: Pamir front thrust, TFF: Taras-Fergana fault, NNBF: north naryn basin fault.

Materials and methods

We processed SAR data from five ascending tracks (T27, T129, T56, T158, T85) and four descending tracks (T107, T34, T136, T63) acquired by the Sentinel-1 satellites between November 2014 and December 2020. In total, we generated 1074 single-look interferometric pairs using Gamma software, covering a area of 790 kilometers in length and 520 kilometers in width covering the TSOB. Subsequently, we processed the time series data using the StaMPS software (Hooper et al., 2004). To account for the long-wavelength and the atmospheric phase screen in each track, we applied the TRAIN package (Bekaert et al., 2015) and the ECMWF ERA5 models. The Line-of-sight (LOS) InSAR rates are depicted in Figure 2a and 2b. To enhance our ability to measure large-scale tectonic plate motion, we employed a correction method for InSAR velocity maps, incorporating the GNSS velocities within the International Terrestrial Reference Frame (ITRF) framework, as shown in Figure 2c and 2d.

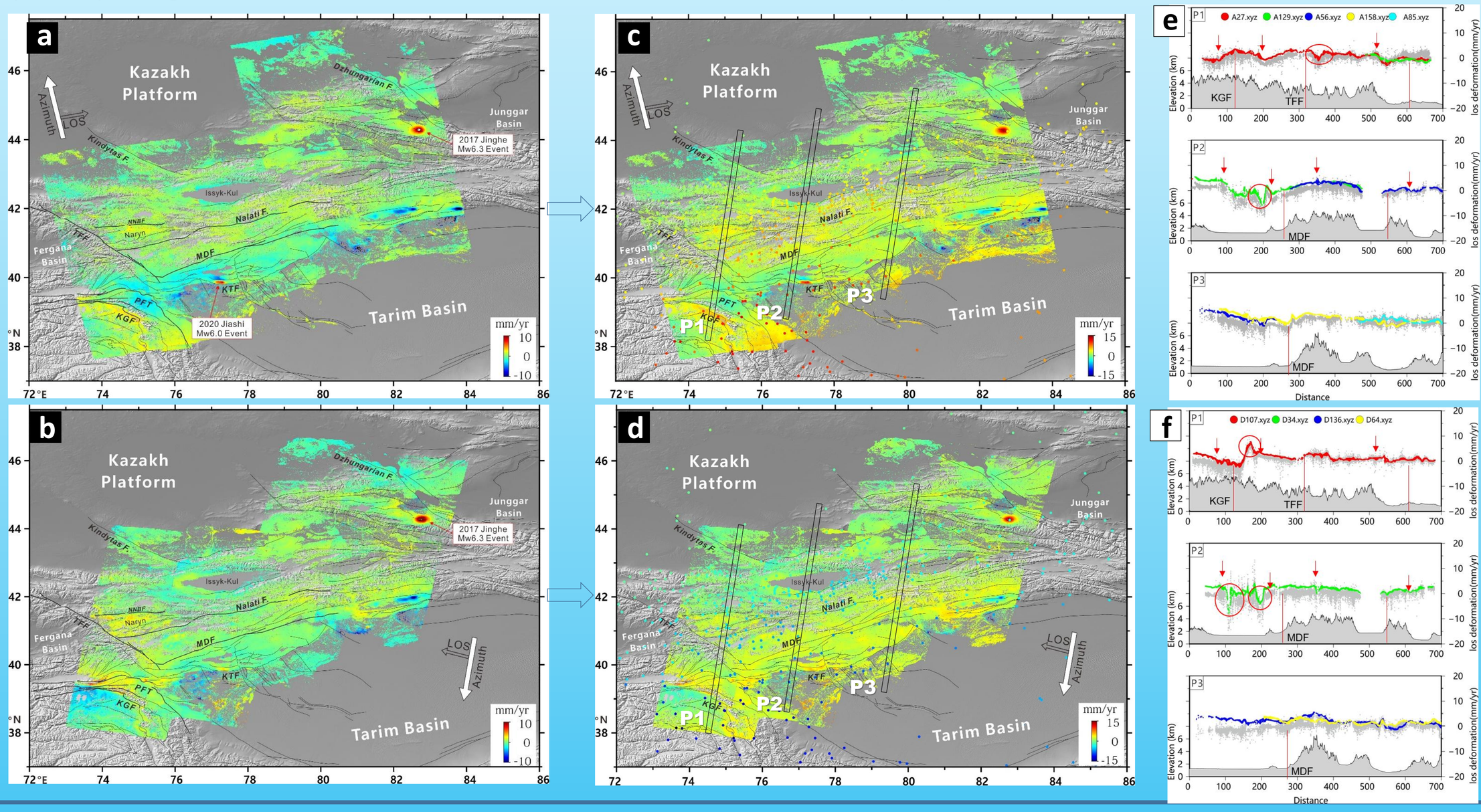

Figure 2. the LOS velocity map of the ascending (a,c) and descending tracks (b,d). (e) and (f) presents three profiles of the ascending and descending tracks respectively. Positive motion is toward the satellite. Black lines represent fault traces. The intersecting black and white arrows indicate satellite flight and look directions. The dots in (c,d) represent GNSS data projected onto the LOS direction of the ascending and descending tracks. The colored dots in the (e,f) are the corrected InSAR data, the gray dots are the uncorrected data, and the terrain profiles are in gray at the bottom.

Conclusion

By combining InSAR and GPS measurements, we have demonstrated that tectonic deformation within the TSOB is non-uniformly distributed. The convergence across the Tianshan ranges averages between 15 and 24 mm/yr. Notably, the largest deformation gradient occurs in the junction area between South Tianshan and Pamir, accounting for approximately 68% of the total convergence deformation. Within this region, the Kashi fold-thrust belt emerges as the most active unit. South Tianshan, on the other hand, exhibits relatively stable characteristics without sharp deformation gradients. In the northern part of South Tianshan, deformation disperses across a network of intermountain active structures and depression basins. This deformation in the TOSB gradually diminishes from west to east and from south to north as one moves farther away from the Pamir Plateau. As a significant fault within South Tianshan, the Maidan fault continues to experience both strike-slip and thrust motions. Our modeling results indicate a dip-slip rate of 6.2–6.4 mm/yr within the shallow flat décollement layer.